Available online at www.sciencedirect.com

jmr&t Journal of Materials Research and Technology

journal homepage: www.elsevier.com/locate/jmrt

Original Article

Novel, injection molded all-polyethylene composites for potential biomedical implant applications

László Mészáros [a,b,*], Balázs Tatár [a], Krisztina Toth [c], Anna Földes [d], Krisztina S. Nagy [c], Angela Jedlovszky-Hajdu [c], Tünde Tóth [e,f], Kolos Molnár [a,b]

[a] Department of Polymer Engineering, Faculty of Mechanical Engineering, Budapest University of Technology and Economics, Műegyetem Rkp. 3, H-1111, Budapest, Hungary
[b] MTA-BME Research Group for Composite Science and Technology, Műegyetem Rkp. 3, H-1111, Budapest, Hungary
[c] Laboratory of Nanochemistry, Department of Biophysics and Radiation Biology, Semmelweis University, Nagyvárad Tér 4, H-1089, Budapest, Hungary
[d] Department of Oral Biology, Semmelweis University, Nagyvárad Tér 4, H-1089, Budapest, Hungary
[e] Institute for Energy Security and Environmental Safety, Centre for Energy Research, Konkoly-Thege Miklós út 29-33, H-1121, Budapest, Hungary
[f] Department of Organic Chemistry and Technology, Faculty of Chemical Technology and Biotechnology, Budapest University of Technology and Economics, Szent Gellért Tér 4, H-1111, Budapest, Hungary

ARTICLE INFO

Article history:
Received 29 October 2021
Accepted 9 January 2022
Available online 15 January 2022

Keywords:
Self-reinforced composite
Biomaterial
Gamma irradiation
Injection molding
Cross-linked polyethylene

ABSTRACT

This study aimed to create a self-reinforced composite material that can be processed by injection molding and other standard thermoplastic processing techniques and can be potentionally used as implant material. Self-reinforcement in biomaterials is desirable because it does not compromise biocompatibility and improves biofunctionality through improved mechanical performance. Self-reinforced composites can be currently processed by specialized, expensive and unproductive methods; hence we aimed to create a simpler processing alternative that works with biocompatible materials. We combined a high-density polyethylene matrix with high-performance polyethylene (Dyneema®) fibers. Before making the composite structure, the fibers were cross-linked by gamma irradiation to prevent their melting and maintain their structural integrity. The cross-linked fibers withstood the compounding by twin-screw extrusion and the subsequent injection molding. The effect of the irradiation dose on the processability, crystallinity, morphology, mechanical performance and cytotoxicity was investigated. We found that adding 20 m% of 200 kGy irradiated Dyneema® fibers increased the tensile modulus by 22.0%, the tensile strength by 71.1%, while both the composite and its constituents were all found to be biocompatible. The 41.1 MPa tensile strength, the 1.62 GPa tensile modulus, and the 64 Shore D hardness is quite similar to those of ultra-high molecular weight polyethylene,

* Corresponding author.
E-mail address: meszaros@pt.bme.hu (L. Mészáros).
https://doi.org/10.1016/j.jmrt.2022.01.051
2238-7854/© 2022 The Author(s). Published by Elsevier B.V. This is an open access article under the CC BY license (http://creativecommons.org/licenses/by/4.0/).

which is widely used in implants. Still, the material introduced in this paper shows no issues with the melt flow characteristics. These achievements are similar to other self-reinforcing methods, but the manufacturing method presented here can be economically realized on widely available processing technologies and machines.

© 2022 The Author(s). Published by Elsevier B.V. This is an open access article under the CC BY license (http://creativecommons.org/licenses/by/4.0/).

1. Introduction

Replacing dysfunctional body parts has been an integral part of medicine since ancient times. As structural materials evolved, so did biomaterials, in place of the early organic materials, like wood; metals, then later polymers and engineered ceramics came into use [1,2].

Nowadays, alongside novel manufacturing technologies [3] and various alloys, biocompatible polymers and polymer composites are at the forefront of biomaterial research [4].

Potential and existing applications include joint replacements and also applications where high load-bearing is necessary. These include but are not limited to implant stems, spinal and trauma implants that require polymers with high strength and stiffness close to that of human bone [5]. Ultra-high molecular weight polyethylene (UHMWPE) is widely used in joint replacements because of its chemical inertness, wear resistance, and mechanical properties, which are more favorable than that of different polyethylene grades [6].

Brostow et al. [7,8] characterize the brittleness (B) as $B = 1/\varepsilon_b \cdot E'$, where $\varepsilon_b \cdot$ is the elongation at break and E' is the storage modulus. For polyethylene, this value is one of the lowest among the polymers tested in their study, meaning that polyethylene is a highly ductile material.

The bottleneck in processing UHMWPE is its high melt viscosity, and therefore applying classical thermoplastic processing methods such as extrusion or injection molding is exceptionally challenging [9,10]. To improve the dimensional accuracy of the product, machining can be necessary, which significantly increases the cycle time and the costs of manufacturing.

A promising way of improving material properties without compromising biocompatibility is self-reinforcement [2]. In self-reinforced composites, both the reinforcing structure and the embedding matrix are made of the same material. As a result, self-reinforced composites are less prone to sudden and catastrophic failures, cracking and delamination (the latter is only relevant at layered structures) [11–14].

Most of the self-reinforcing technologies do not allow complex and bulky 3D geometries, but shell structures instead. There are also various techniques realized by special, modified injection molding machines or extruders [15,16], but their application is very limited.

Megremis et al. [17] produced hot compacted, self-reinforced composites from UHMWPE. For this, they used gel spun, high-performance UHMWPE (Spectra®) fibers. After hot compaction, the composites had ten times higher tensile strength and modulus than the UHMWPE reference. Huang et al. [9,18] blended ultra-low molecular weight polyethylene (ULMWPE) with neat UHMWPE and gamma-irradiated UHMWPE, which helped keep the material's structural integrity. They used shear-controlled orientation in injection molding (SCORIM) to produce specimens from these materials. In the irradiated case, they achieved positive results in the wear rate and fatigue resistance as well as an increase of 194% in the tensile strength and a 58% increase in the tensile modulus.

From the literature, it is clear that high-performance UHMWPE fibers can be used to increase the strength and stiffness of PE through self-reinforcement very efficiently.

A possible method of widening the processing window is the cross-linking of the reinforcing fibers. Such a structure can retain material cohesion even upon crystalline melting, such as in the case of the composites produced by Huang et al. [18]. One of the most popular ways to generate cross-linking is high energy irradiation, which we chose to apply in this study. Compared to other methods, like chemical cross-linking, it is favorable because it can be carried out without the need to melt or dissolve the polymer, i.e., the UHMWPE fibers. On the other hand, irradiation can also deteriorate mechanical properties because cross-linking can decrease molecular orientation. Besides, irradiation inevitably causes some degree of degradation in the polymer [19].

Based on all these aspects, this research aimed to produce injection moldable and biocompatible polyethylene composites, typically for bone replacement implants. We wanted to bypass the bottleneck of UHMWPE melt-processing and create a feasible, large-scale, and cost-effective way of processing. Therefore, we chose injection molding that is widely available for large-scale production [20]. To achieve that aim, we chose high-density polyethylene (HDPE) as matrix and gamma irradiation cross-linked UHMWPE (Dyneema®) fibers as reinforcement. We elaborated the method of making such injection molded, self-reinforced composites, then characterized their mechanical performance and biocompatibility using human fibroblasts.

2. Materials and methods

2.1. Materials used and gamma irradiation treatment

We used Tipelin BA 550–13 type HDPE supplied by MOLGroup Chemicals (Hungary) as matrix material. It has a melt flow index of 0.35 g/10 min (190 °C/2.16 kg) and a recommended processing temperature range of 180–220 °C. The reinforcing material used was a high-performance UHMWPE fiber, namely Dyneema® SK75 fiber with a linear density of 400 dtex, produced by DSM (the Netherlands) company by gel spinning process. According to the material's technical datasheet, it has a nominal crystal melting temperature range of 144–152 °C.

The Dyneema® fibers were manually cut into 8–10 mm long strands. The fibers were subjected to gamma irradiation in hermetically sealed PE bags. The samples were irradiated with a ^{60}Co gamma source (panoramic type SS-01 γ-irradiation facility) at ambient temperature at a dose rate of 2 kGy/h. The chopped strand fibers and longer pieces of the filament yarns were irradiated with doses of 100 kGy, 200 kGy and 300 kGy, and a non-irradiated reference yarn sample was also set aside.

2.2. Differential scanning calorimetry for the fibers

To investigate the thermal and crystalline properties of the fibers, differential scanning calorimetry (DSC) measurements were conducted on the neat and irradiated fiber samples with a TA Instruments (New Castle, USA) Q2000 type device. The 5–7 mg precisely weighed samples were heated from 0 °C to 210 °C with a constant heating and cooling rate of 20 °C/min. Five DSC measurements were conducted on each Dyneema® fiber sample with differing irradiation doses to avoid faulty measurements and outlier values. The melting enthalpy of the 100% crystalline polyethylene (ΔH_m^{100}) was taken as 293 J/g [21]. The degree of crystallinity was calculated using Equation (1), where ΔH_m is the melting enthalpy, measured from the melting curve with a sigmoid virtual baseline.

$$\chi = \Delta H_m \cdot 100 / \Delta H_m^{100} \quad (1)$$

2.3. Single fiber tensile tests

Tensile tests were carried out on both the irradiated and non-irradiated single fibers using a Zwick-Z005 (Ulm, Germany) type tensile testing machine. Pieces of single fibers taken from the filament yarns were fixed to paper frames by adhesive tape for better handling. The fiber diameters were measured individually before the tests with the aid of an Olympus BX51M (Tokyo, Japan) type light microscope equipped with a digital camera. A grip-to-grip separation was 25 mm, corresponding to the paper frame size. After gripping the fiber together with the frame, the edges of the paper frame were cut; hence only the fiber was tested. A testing speed of 2 mm/min was used until the fiber broke. The force was measured with a load cell having a measurement limit of 20 N and a resolution of 0.001 N. The Young's modulus was calculated as the slope of the tangent line at the steepest part of the curve. For the un-irradiated fibers, to prevent them from slipping from the grip, the fibers were tied multiple times around the holding frame. A total number of 10 fibers were tested for each sample group.

2.4. Determining the gel content by soxhlet extraction

Soxhlet extraction was performed on the irradiated fibers to determine their gel content and confirm cross-linking. The experiment was done on a BEHR Labor Technik (Düsseldorf, Germany) R 256 S type extractor with isomeric xylene mixture as solvent. Before the experiment, the highly crystalline fibers were hot-pressed into thin sheets at 160 °C and then slowly cooled down to recrystallize them. This step was necessary to decrease the degree of crystallinity and the crystalline melting temperature and enhance the dissolution characteristics [22]. The chemical cross-links formed by the gamma irradiation were unaffected by this step [23]. We dried the samples at 60 °C for 3 h before measuring their mass, both before and after the extraction. We did the Soxhlet extraction experiments in triplicate.

2.5. Processing of self-reinforced composites

The resin and the chopped and irradiated fibers were compounded on a Labtech (Samut Prakan, Thailand) LTE 26–44 twin-screw extruder at zone temperatures of 170 °C–190 °C, gradually increasing from the hopper to the die. The applied double-hole filament die temperature was also set at 190 °C. The fiber content was chosen to be 20% w/w because higher content might lead to issues in compounding. The material flow was cooled on air and granulated on a Labtech LZ-120/VS granulator. We made four types of granules, respectively containing the 0, 100, 200, 300 kGy irradiated fibers.

The granules containing the irradiated fibers were then fed into an Arburg (Loβburg, Germany) Allrounder 420C injection molding machine. Standard, 4 × 10 mm^2 1A type dumbbell specimens, in accordance with ISO 527, were injection molded from the four types of composite granules (containing the irradiated or the non-irradiated fibers). Besides, neat HDPE resin was also injection molded as a reference. For the neat HDPE, 190 °C temperature, 40 cm^3/s injection speed, 2000 bar filling pressure, and 1200 bar packing pressure produced proper samples. The composites needed to be processed at 200 °C to achieve full cavity filling, an injection speed of 55 cm^3/s, filling pressure of 2000 bar and a packing pressure of 1500 bar were used.

Depending on the adsorbed irradiation doses of the fibers, we named these injection molded samples (Fig. 1) as 0 kGy composite, 100 kGy composite, and so on. Upon injection molding, we did not anneal the samples.

2.6. Differential scanning calorimetry for the composites and the reference

DSC measurement was also conducted on the injection molded all-PE composites and on the reference specimen to investigate their thermal and crystalline properties and

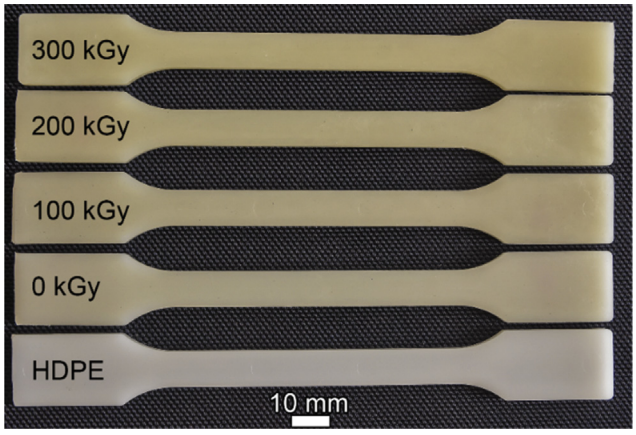

Fig. 1 – The injection molded specimen reinforced with fibers irradiated with different absorbed doses.

compare them with the properties of the fibers. This time only a single measurement was conducted for each sample. The device and the cycle were the same as presented in 2.2. The melting enthalpy of the 100% crystalline PE was again taken as 293 J/g [21], and (1) was used to calculate the degree of crystallinity from the melting enthalpy determined by using a sigmoid virtual baseline.

2.7. Tensile and hardness tests of composites

The tensile tests were carried out on the dumbbell specimens with a Zwick Z005 tensile tester equipped with a 5 kN load cell. A grip to grip separation of 110 mm and a testing speed of 50 mm/min were used. When evaluating the tests, the Young's modulus was calculated as the slope of the tangent line at the steepest part of the curve. From each sample type, five specimens were tested. The specific fracture energy was calculated by numerically integrating the area under the measured tensile curve.

The Shore-D hardness tests were carried out on a Zwick 3103 IHRD Micro Compact III microhardness tester. Five specimens of each dumbbell specimen type were tested.

2.8. Electron microscopy

The adhesion between the fibers and matrix was evaluated by inspecting the fracture surface of the composite after the tensile tests. In addition, some specimens that did not completely fill the mold cavity at the injection molding process (when finding the proper injection molding parameters) were also investigated. Before inspecting the samples, they were sputtered with a thin gold layer. For this purpose, scanning electron microscopic (SEM) images were taken with a JEOL (Tokyo, Japan) JSM 6380 type microscope.

2.9. Cytotoxicity

To characterize the biocompatibility of the materials, we performed cytotoxicity tests. The pieces of the injection-molded specimens were investigated and their components: both the matrix (HDPE granulates) and the fibers (irradiated or non-irradiated). Even though the matrix of the composite was non-irradiated, we also tested irradiated HDPE granules. That was to be able to better compare the behavior of HDPE and UHMWPE in regards to cytotoxicity.

Minimal Essential Medium Eagle (Gibco, USA), Foetal Bovine Serum (FBS) (Gibco, USA), L-glutamine (Gibco, USA), penicillin-streptomycin mix (Gibco, USA), Non-Essential Amino Acids (NEAA) (Gibco, USA), Minimal Essential Medium, no glutamine, no phenol red (Gibco, USA), WST-1 [2-(4-Iodophenyl)-3-(4-nitrophenyl)-5-(2,4-disulfophenyl)-2H-tetrazolium] (Roche, Switzerland), trypsin–EDTA (Gibco, USA), Dulbecco's Phosphate Buffered Saline (PBS) (Lonza), ClO_2 (Solvocid, Solumium Kft., Hungary) were used for the cytotoxicity characterization.

First of all, 0.5 cm pieces were cut from the molded specimens and weighed. According to the weight ratios of the components in the composite specimens (20 m/m% fiber content), one-fifth of this weight was measured from the fibers and four-fifth of this weight was measured from the HDPE granulate.

The appropriate amount of samples were placed into a 12 well cell culture plate, they were sterilized in ClO_2/PBS (1:100) solution for 1 h, and after that, they were soaked into a cell culture medium for 24 h.

3 ml medium was added to the reference specimen of 0.2 g. To get equal final concentrations in the case of each sample, the volume of the added cell culture medium was proportional to the weight ratios of the samples, according to Table 1.

During the cytotoxicity study, we followed Part 5 ("Tests for *in vitro* cytotoxicity") of the ISO 10993 Standard („Biological evaluation of medical devices"). 155BR human fibroblast (ECACC 90011809, Sigma–Aldrich, USA) cells were seeded at a density of 10 000 cells/cm^2 into 96 well plates in 100 μl cell culture medium at 37 °C, 5% CO_2, 100% humidity. The culture medium consisted of Eagle's Minimal Essential Medium supplemented with 15% (V/V) FBS, 2 mM L-glutamine, 1% (V/V) NEAA, 100 units/ml penicillin, and 100 mg/ml streptomycin. After one day of culturing, the medium was removed, and 100 μl supernatant of the PE samples and composites was added to each well.

After 24 and 72 h of treatment with the supernatants, WST-1 cell proliferation reagent was diluted at 1:20 dilution with Minimal Essential Medium without Phenol Red. 100 μl of the mixture was applied in each well for 4 h at 37 °C. The absorbance of the generated formazan molecules from WST-1 was measured by a fluorescent microplate reader (Model 3550, Bio-Rad Laboratories, Japan) at 450 nm with 650 nm reference wavelength. Wells containing only the reagent but no cells were used as blank while untreated cells were used as control.

The morphology of the cells was also observed by phase-contrast microscopy with a 4× objective lens (Nikon Eclipse TS100, Nikon, Japan) after 24 and 72 h of the treatments. Images were taken with a high-performance CCD camera (COHU, USA) applying the Scion image software.

Statistical evaluation of the viability data was carried out using the Kruskal–Wallis nonparametric ANOVA followed by a median test. A difference was considered as statistically significant if $p < 0.05$.

Table 1 – Details of the materials used in the cell experiments (at the composite samples, only the reinforcing fibers were irradiated)

	Composite	Fibers	HDPE
Reference			
Weight of the sample [g]	0.2031	0.0471	0.1654
Volume of the medium [ml]	3.000	3.479	3.054
100 kGy dose			
Weight of the sample [g]	0.1455	0.0291	0.1182
Volume of the medium [ml]	2.149	2.149	2.182
200 kGy dose			
Weight of the sample [g]	0.1553	0.0311	0.118
Volume of the medium [ml]	2.294	2.294	2.179
300 kGy dose			
Weight of the sample [g]	0.1745	0.0349	0.1385
Volume of the medium [ml]	2.578	2.578	2.557

3. Results and discussion

3.1. DSC measurements for the fibers

DSC measurements can reveal valuable information about the thermal and crystalline properties of these all-PE materials. We started our investigations with the fibers. Both heating cycles provide information about the effect of the irradiation. The results of the first heating cycle show the impact of the irradiation itself on crystallinity. In contrast, the second heating cycle shows how the fibers behave upon a heat treatment similar to what happens during the processing.

Fig. 2 shows representative DSC curves of the fibers for each dose, and Table 2 shows the average results of the measurements and their standard deviation.

The crystalline melting temperatures and the degrees of crystallinity were much lower in the case of all the second heating cycles (Fig. 2(b)). At the manufacturing of the fibers, fiber drawing oriented the molecules to a great degree, increasing the degree of crystallinity. Here, a different crystalline structure forms than at the gel spinning because when the polymer crystallizes after the first cycle of the DSC test, it does so under no mechanical stress.

As a result of the irradiation, the crystalline melting temperature decreased in both heating cycles. The decrease occurs because the crystalline structure is weakened by the degradation of the constituting molecules and the strain imposed by the cross-links in the surrounding amorphous regions. The degree of crystallinity (χ) increased in both heating cycles when the fibers were irradiated. The most significant changes in properties occurred after absorbing the first 100 kGy of dosage. The increase in crystallinity in the second heating cycle indicates substantial degradation occurring in the material. The shorter molecules are more mobile and can form crystalline structures more easily than longer molecules. The slight drop in crystallinity at 200 kGy can indicate cross-linking becoming more dominant, as cross-links impede crystallization. In the first heating cycles, the increase in the degree of crystallinity is much smaller, and the standard deviations overlap. It can be a result of the recombination of free radicals trapped inside the crystalline structures. As they combine, they can hinder the melting of the crystalline parts resulting in a higher enthalpy required to melt them.

Table 2 – The crystal melting temperatures (T_m) and degrees of crystallinity (χ) obtained from DSC measurements of the fibers

Sample	T_m [°C] (1st heating)	χ [%] (1st heating)	T_m [°C] (2nd heating)	χ [%] (2nd heating)
neat fiber	147.5 ± 0.4	80.6 ± 4.1	135.3 ± 0.4	44.6 ± 2.0
100 kGy fiber	143.4 ± 0.4	85.6 ± 3.5	135.2 ± 0.3	60.4 ± 1.0
200 kGy fiber	142.5 ± 0.4	85.6 ± 3.4	134.2 ± 0.9	58.3 ± 1.2
300 kGy fiber	141.7 ± 0.9	87.3 ± 3.8	133.5 ± 0.4	58.7 ± 0.6

3.2. Soxhlet extractions

Soxhlet extraction of irradiated UHMWPE samples in xylene has been reported previously, for example, in references [25–27]. However, these cannot be directly equated to Dyneema® fibers having a substantially high degree of molecular orientation and a higher degree of crystallinity. When we tested the Dyneema® fibers without a preceding hot pressing, they did not dissolve in boiling xylene at 139 °C. That is likely a result of the high crystallinity of the fibers, which the solvent could not infiltrate. As we observed at the first DSC heating cycle, the fibers remain semi-crystalline at this temperature. The degree of crystallinity greater than 80% means that the solvent cannot unravel the crystalline domains through swelling the amorphous ones. After recrystallizing the samples through hot pressing, we get crystalline properties like those obtained at the second DSC heating cycle. As the T_m decreased below the boiling point of xylene and the degree of crystallinity also reduced, the samples could be dissolved. However, it is clear that Soxhlet extraction in xylene is not entirely suited to Dyneema® fibers, as because of the high molecular weight, the neat samples could not be dissolved completely. The un-irradiated samples had a relatively high gel content (Table 3.) due to the high entanglement rate resulting from the high molecular weight. The gel content decreased in the case of the irradiated samples. The experiment has a high sensitivity for impurities and temperature changes that resulted in high standard deviations. The deviation is particularly high in the case of the 200 kGy samples, and besides, deviations overlap. The overall decrease is likely

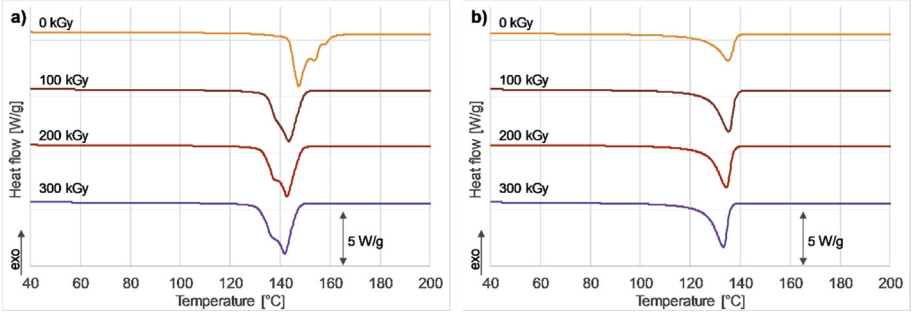

Fig. 2 – The DSC curves from the first a) and the second b) heating cycle for Dyneema® irradiated fibers.

Table 3 – Gel fractions from the Soxhlet extractions for hot-pressed Dyneema® fibers with different absorbed doses

Sample	Gel fraction [%]
0 kGy heat-treated fibers	46.5 ± 15.0
100 kGy heat-treated fibers	23.1 ± 4.7
200 kGy heat-treated fibers	31.4 ± 12.2
300 kGy heat-treated fibers	16.1 ± 2.2

because of the molecular weight-reducing effect of chain-scission during the irradiation. The role of the entanglements decreases when a polymer is irradiated (chain-scission); still, there is a measurable gel content at high doses that can not be the result of entanglements but instead of cross-linking.

3.3. *Single fiber tensile tests*

The single fiber tensile tests were carried out on fibers irradiated with different doses and non-irradiated fibers. In the case of the non-irradiated samples, some slipping of the fibers between the grips occurred, and we were not able to completely eliminate that (Fig. 3). Besides the slipping, however, the tests ended with fiber breakage. The measured tensile strength of the non-irradiated fibers corresponds well with the value presented in the technical datasheet of the material, but the elongation at break is higher due to this slipping. Despite the degradation and cross-linking caused by the gamma irradiation treatment, the strength and modulus of all fibers greatly exceeded those of the matrix material and thus were well suited for being fiber reinforcement.

The tensile strength and elongation at break consistently decreased due to the irradiation (Table 4). The Young's modulus decreased for the irradiated samples but remained high for different doses. Fiber tensile tests often result in higher standard deviations because of the smaller cross-section. The standard deviations of Young's moduli considerably overlap, especially for the irradiated samples; thus, these changes cannot be considered significant. Taken

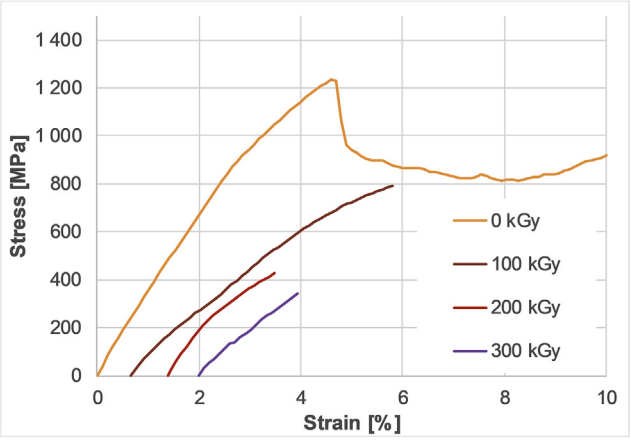

Fig. 3 – Representative tensile curves of Dyneema® fibers with different absorbed doses (the curves are shifted horizontally for better visibility).

Table 4 – The results of the single fiber tensile test of Dyneema® fibers with different absorbed doses

Sample	Tensile strength [MPa]	Strain at break [%]	Young's modulus [GPa]
0 kGy fiber	2797 ± 463	13.59 ± 4.34	29.4 ± 5.1
100 kGy fiber	735 ± 153	2.14 ± 0.53	21.6 ± 4.6
200 kGy fiber	393 ± 114	0.70 ± 0.18	25.9 ± 4.9
300 kGy fiber	248 ± 86	0.41 ± 0.25	20.8 ± 6.5

together with the solubility results, it is possible that the stand-out results of the 200 kGy samples indicate the dominance of cross-linking at this dose. Some decrease in mechanical properties often occurs due to irradiation, especially in the case of a high degree of crystallinity. The degradation taking place during irradiation lowered the molecular weight and damaged the crystalline domains. That created weak spots in the material, which could cause failure more quickly. Still, the fibers lost minor stiffness and modulus because of this quicker failure and inhibited the load's dispersion. Despite the decrease in these properties, the fibers remained considerably stronger and stiffer than the HDPE matrix itself. Therefore it still had plenty of reinforcing potential.

3.4. *DSC measurements for the composites*

For simplicity, we name the samples with the dose absorbed by the fibers before the composite preparation, e.g., '100 kGy composite' refers to an injection molded composite with HDPE matrix and 100 kGy dose gamma-irradiated Dyneema® fibers. When comparing the DSC results of the individual fibers and the composites, we must keep in mind that the fibers in the composites are recrystallized during the injection molding. Therefore, we instead compare the first heating cycles for the composites with the second heating cycles for the individual fibers. The T_m of the neat HDPE specimen is slightly lower than that of the individual fibers. The T_m values of the composites lie between the T_m values of the matrix and the fibers. There is only a single peek in the curve indicating that the fibers and the matrix did not form wholly different crystalline domains, but instead, their crystalline structures influenced each other, and were very similar (Fig. 4).

At the injection molded all-PE composites, T_m did not change significantly or consistently due to the fibers' irradiation, unlike at the fibers' measurements. In the case of the second DSC heating cycle for the individual fibers, the effects of irradiation on the T_m were much lessened, compared to the first cycle. These fibers were then added in relatively low content, 20 wt%, to the matrix resin. In such a low concentration, the small changes in the fibers did not affect the composites significantly (Table 5).

The χ of the HDPE specimen was somewhat higher than that of the recrystallized non-irradiated fibers, therefore when HDPE was reinforced with the non-irradiated fibers, χ decreased slightly. As an effect of the irradiation on the reinforcing fibers, the χ of the composites increased slightly for

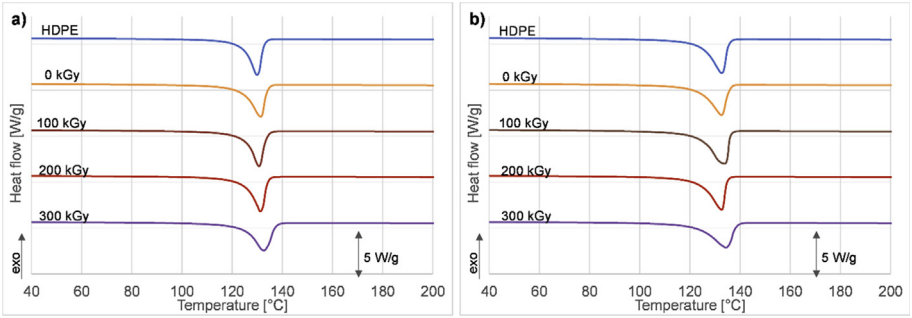

Fig. 4 – The DSC curves from the first a) and the second b) heating cycle for the composites reinforced with Dyneema® fibers irradiated with different doses.

both heating cycles. This, in some part is simply the result of the fibers themselves having an increased degree of crystallinity. Besides, if cross-linked fibers could provide crystallization nuclei for the matrix, accounting for a greater than proportional increase.

There is a slight but consistent increase for both the χ and the T_m values of the second heating cycle compared to the first, showing that the polymer crystallized differently under stress in the mold, then under no stress.

3.5. *Composite tensile tests*

Fig. 5 shows characteristic tensile curves for each injection molded composite sample, while Table 6 Contains the average results and standard deviations for each sample.

The values, in this case, had a smaller standard deviation than in the case of the fiber tensile test. As a result of the non-irradiated fiber reinforcement, the HDPE lost some of its ductility. The specific fracture energy and the elongation at break decreased, while the tensile modulus remained approximately the same, and the tensile strength slightly increased. The reinforcing effect in the case of non-irradiated fibers was not very effective. Without the gamma-irradiation treatment, the UHMWPE had a linear molecular structure that completely melted during the processing. As a result of thorough mixing of the fibers by twin-screw extrusion followed by injection molding, we assume that we obtained a blend of UHMWPE and HDPE. When the fibers were irradiated with varying doses, the composite's characteristics changed substantially. The tensile strength and modulus increased, while the elongation at break decreased considerably. It is because cross-linked fibers kept their integrity better in the composite, thus could reinforce more effectively. The properties of the individual fibers had a lesser impact than their ability to withstand the processing. Above an absorbed dose of 200 kGy, further irradiation up to 300 kGy did not impact the tensile properties significantly. These results indicate that the cross-linking that took place up to the 200 kGy dose was sufficient for the fibers to keep their integrity. Further irradiation can only cause changes (i.e., slight degradation) in the fibers themselves, not in their structure within the composite. In the case of the 200 kGy composite samples, the tensile modulus and the tensile strength increased by 23% and 71%, respectively. Compared to the application of non-irradiated fibers, the increase is still

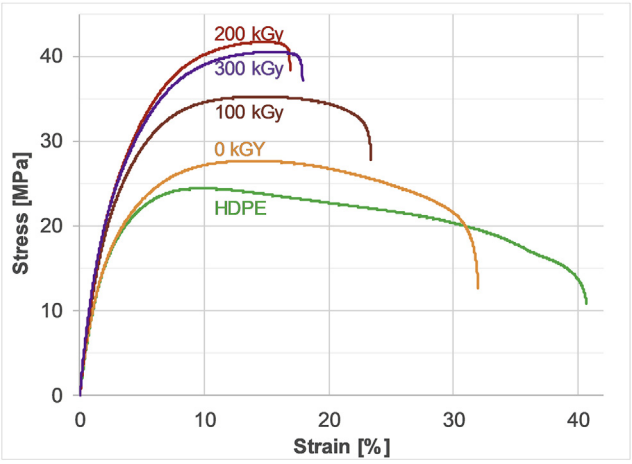

Fig. 5 – Representative tensile curves of the reference and the composite samples.

Table 5 – The crystal melting temperatures (Tm) and degrees of crystallinity (χ) obtained from DSC measurements of the composites

Sample	T_m [°C] (1st heating)	χ [%] (1st heating)	T_m [°C] (2nd heating)	χ [%] (2nd heating)
HDPE specimen	129.9	52.7	132.7	59.3
0 kGy composite	131.4	52.1	132.6	55.5
100 kGy composite	130.7	53.8	133.0	59.1
200 kGy composite	131.4	53.9	132.7	56.2
300 kGy composite	132.7	52.6	134.4	55.9

Table 6 – The results of the tensile tests on composite samples and the HDPE reference

Sample	Tensile strength [MPa]	Strain at break [%]	Young's modulus [GPa]	Specific fracture energy [J/mm^3]
HDPE (no fibers)	24.0 ± 0.2	44.9 ± 6.5	1.32 ± 0.04	8.4 ± 1.3
0 kGy composite	27.3 ± 0.2	29.2 ± 2.9	1.33 ± 0.03	6.0 ± 1.1
100 kGy composite	34.3 ± 0.6	29.0 ± 4.2	1.35 ± 0.03	7.5 ± 0.6
200 kGy composite	41.1 ± 0.7	17.1 ± 1.3	1.62 ± 0.05	5.1 ± 0.2
300 kGy composite	39.8 ± 0.7	16.8 ± 2.6	1.61 ± 0.02	5.1 ± 0.4

Table 7 – The results of the hardness tests

Sample	Shore D hardness [-]
HDPE	61.1 ± 1.7
0 kGy composite	62.0 ± 1.8
100 kGy composite	63.2 ± 2.1
200 kGy composite	64.4 ± 1.3
300 kGy composite	65.5 ± 0.8

considerable: 22% and 50.5% in these properties. That is because non-irradiated fibers were able to melt during the processing, but gamma-irradiation helped the fibers to maintain their structural integrity. The specific fracture energy was used to characterize the ductility of the specimens. We can see that in accordance with the elongation at break, ductility decreased when reinforced with the fibers. When irradiated with 100 kGy, the ductility increased, but the specimen became more brittle at higher doses.

The composite samples' measured tensile properties are worth being compared to UHMWPE currently used in implants. For example, Lombardo et al. [28] reported 35–43 MPa ultimate strength, 8.6–11.4% strain at break, 71–120 MPa tensile modulus, depending on quenching and annealing. Bellare et al. [29] reported 45 MPa yield strength, 11% strain at break and a 120 MPa modulus. Wang et al. [30] reported 28 MPa yield strength and 400 MPa Young's modulus for the neat UHMWPE and 31 MPa and 1.4 GPa for 300 kGy gamma irradiation treated annealed UHMWPE.

We can conclude that we obtained a similar strength but a higher modulus and a higher strain at break at all the fiber irradiation doses, without either annealing or further irradiating the samples after the injection molding. The further treatment of the samples is out of the scope of this study.

3.6. *Hardness tests*

The hardness tests showed an increasing Shore D hardness due to fiber reinforcement and the irradiation of the reinforcing fibers (Table 7.). The fibers have increased strength and molecular weight that contribute to the hardness of the composite, compared to the neat HDPE matrix. The increase in hardness as a result of the irradiation is likely a result of cross-linking taking place. The cross-links obstruct molecular motion and deformation, resulting in a harder material. As a comparison, Visco et al. [31] reported a Shore D hardness of 60.9 for UHMWPE.

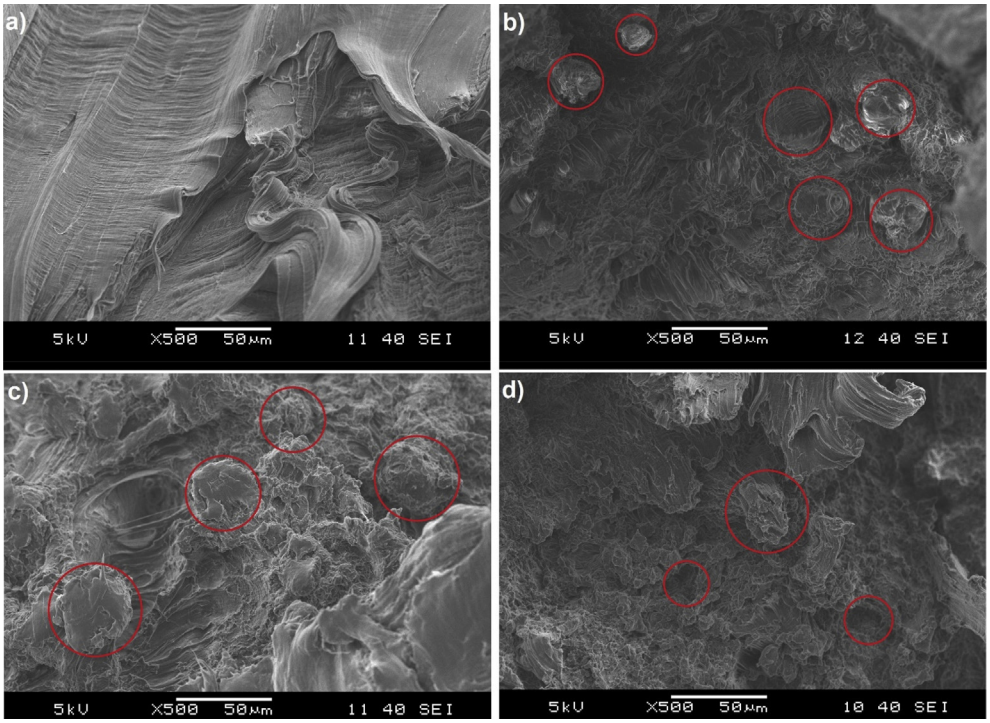

Fig. 6 – SEM images of the tensile tested surfaces of the composites reinforced with Dyneema® fibers irradiated with 0 kGy (a), 100 kGy (b), 200 kGy (c) and 300 kGy (d).

Hardness correlates closely with wear properties. An increase in material hardness indicates more favorable wear properties and creep resistance, which needs further studies in the future.

3.7. Electron microscopy

Fig. 6 shows the fracture surfaces of the composites after the tensile tests. In the case of the composite containing unirradiated fibers (Fig. 6(a)) no fibers can be detected. It means that the fibers melted when the composite was generated, which resulted in a more ductile fracture surface. In the case of the specimens containing irradiated fibers, the fibers are visible (Fig. 6(b,c,d)); hence we can conclude they kept their integrity. We encircled the detected fibers, fiber bundles, and the holes indicating pulled-out fibers with red. It is visible that the matrix well covered the fibers.

For deeper analysis, we investigated the reference materials (HDPE and Dyneema®) and the tensile specimen we received when the injection molding parameters were being set (the cavity was only partially filled). The fracture surface of the unreinforced HDPE (Fig. 7(a)) shows a tough behavior, indicated by the created fibrils. Fig. 7(b) shows the Dyneema® fibers with no treatment. It can be concluded that their diameter is in a similar range as we found in the case of the composites (Fig. 6). In the case of the partial filling, we investigated the region where the polymer melt did not touch the mold surface. Fig. 7(c) shows the sample with fibers irradiated with 300 kGy. We could detect whole fibers sticking out of the surface, also proving that the fibers kept their integrity throughout the processing. Moreover, the matrix connects strongly to the fibers.

3.8. Cytotoxicity tests

To investigate the biocompatibility of the all-PE composites, indirect cytotoxicity experiments were performed applying the 155BR human skin fibroblasts and the extracts of the different types of composite samples and their components using the growth medium of the cells. Fig. 8 demonstrates that the confluency level (the surface area covered with cells) is approximately 50–60% in each case after 24 h-long treatments with the extracts. All of the 155BR cells have an elongated shape, with some processes indicating healthy morphology. However, the cell cultures treated for 72 h with the supernatant of the fiber-type samples have a decrease in density (Fig. 9) in contrast to the other treatments where the confluency is almost 100%. Nevertheless, all cells show healthy morphology at this time, too. The cytotoxicity tests confirmed these observations.

Fig. 10 shows the cytotoxicity results regarding the different sample types (specimen/fiber/granule). After 24 h, none of the samples provoked a significant cell number decrease, which is in good agreement with the phase-contrast microscopic images (Fig. 8). In the case of the treatment with the supernatant of the fiber-type samples, the cells have a slightly reduced viability after 72 h compared to the untreated control (*) (see Fig. 10).

This can be explained by the higher specific surface area of these samples, which can make the potential release of a cytotoxic compound from these fibers faster, which is in good agreement with the literature [32,33]. An increase in the viability between 24 h and 72 h can be observed in the case of each sample type, suggesting that the fibroblast cells could not only survive in the presence of the extracts but also reproduce

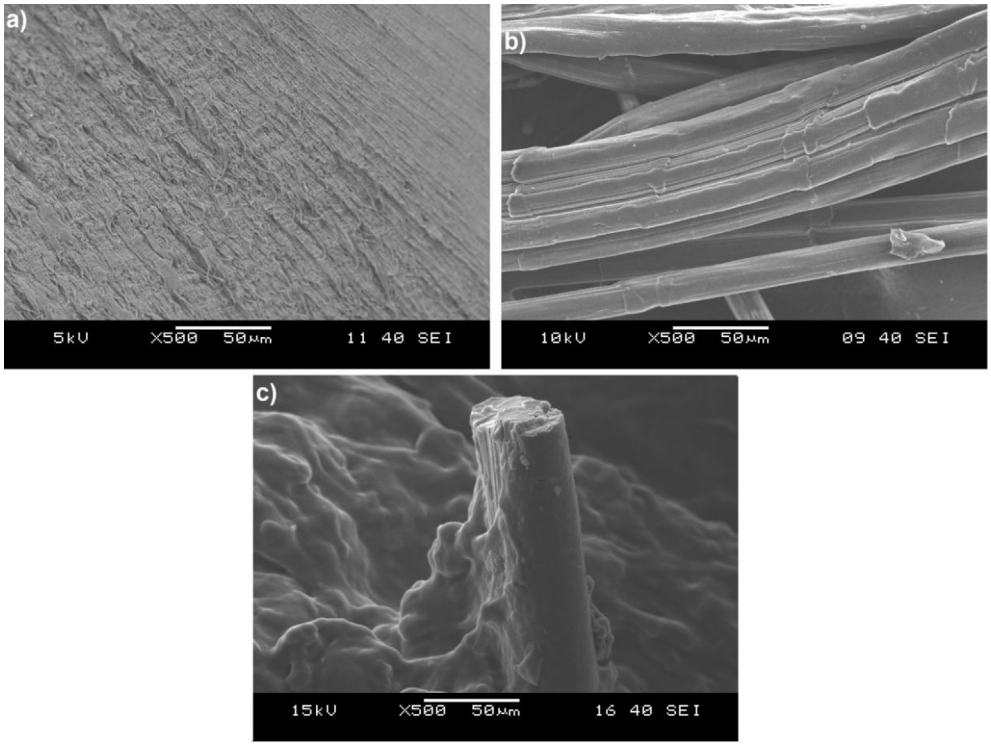

Fig. 7 – SEM images of the tensile tested surface of the HDPE matrix (a), a fiber on the surace of a partially filled specimen (b), Dyneema® fiber bundles (c).

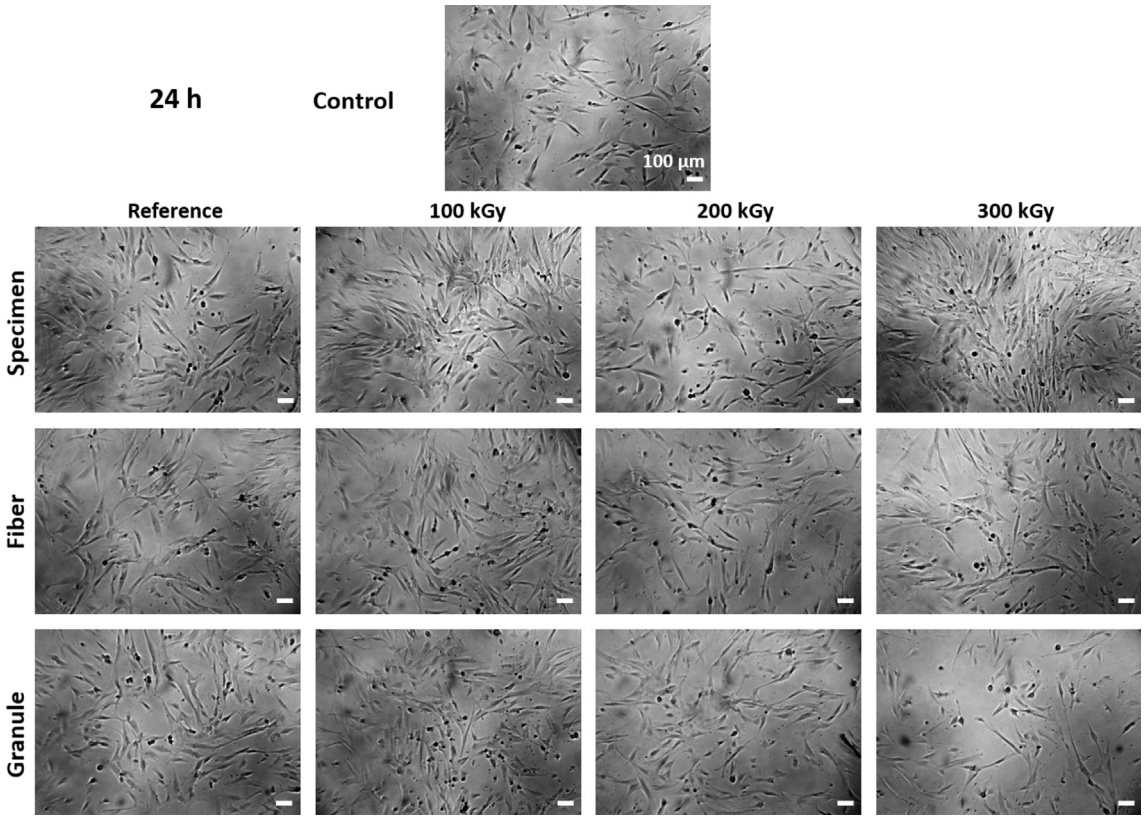

Fig. 8 – Phase-contrast microscopic images of 155BR fibroblast cells growing in the presence of the supernatant of the different sample types (specimen/fiber/granule) for 24 h. The scale bars indicate 100 μm.

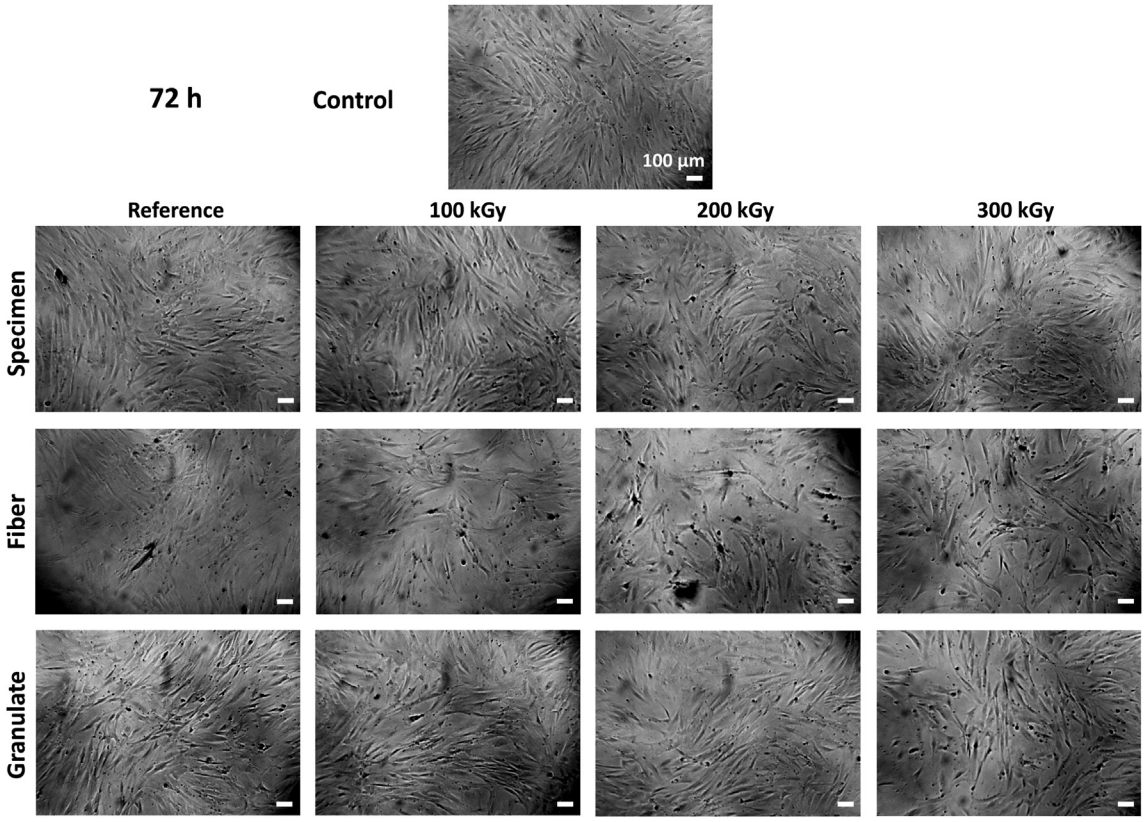

Fig. 9 – Phase-contrast microscopic images of 155BR fibroblast cells growing in the presence of the supernatant of the different sample types (specimen/fiber/granule) for 72 h. The scale bars indicate 100 μm.

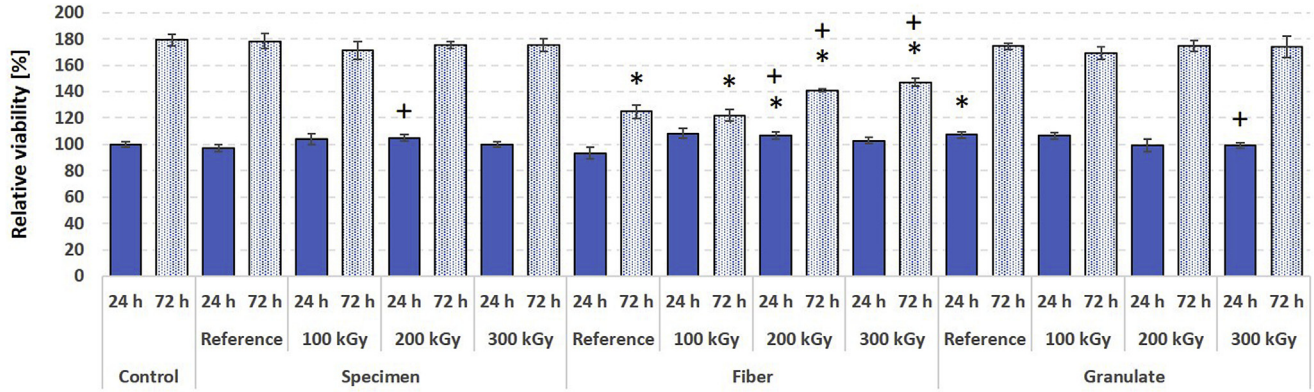

Fig. 10 – Relative cell viability of 155BR human fibroblast cells treated with the supernatants of the different samples for 24 or 72 h. The viability was normalized to the value measured in the case of the control after 24 h. * significant difference ($p < 0.05$) compared to the daily untreated control (24/72 h), + significant difference ($p < 0.05$) compared to the daily (24/72 h) reference of the same sample-type (specimen/fiber/granulate).

themselves (i.e. proliferate). Despite the slight fall of the cell viability in the case of the fiber-type samples, these components are neither toxic for the cells as they may only slightly attenuate the proliferation rate of the cells (Fig. 10).

Thus, based on the phase contrast microscopic images and the cytotoxicity measurements, we can conclude that neither the specimens nor their components proved toxic in this *in vitro* experiment. Since the composition of the cell culture medium and the presence of the human cells simulates the physiological circumstances, we can assume that these self-reinforced PE-based samples would not be toxic when applied *in vivo* as an implant. The biocompatibility of polyethylene and its use as an implant material is well known [34]. Our studies show that this is also the case for self-reinforced polyethylene systems. According to our results, presumably, no toxic by-products will be released from these composite materials when they come into contact with human tissues.

Similar to our results, Firouzi et al. [24] found that extracts of neat UHMWPE fibers reduced the viability of fibroblasts in spite of nylon-coated fibers. In addition, Mamidi et al. [35] also observed that the viability of fibroblast cells was lower in the presence of UHMWPE fibers compared to multiwall carbon nanotube/UHMWPE composites. Taken together, although UHMWPE fibers alone can slightly reduce the viability and proliferation rate of human cells, they show no toxic effect when applied as a component of a composite material. Therefore, our HDPE samples reinforced with UHMWPE fibers having promising mechanical properties would be good candidates as bone implant materials in the future.

4. Conclusions

This study aimed to make self-reinforced biocompatible composites that supposedly can be used as implants. UHMWPE is widely used in implant applications, but its drawback is the difficult and costly processing due to its high melt viscosity. To overcome this issue, we irradiated Dyneema® (UHMWPE) fibers with a ^{60}Co gamma source and embedded those in HDPE matrix composites. This new approach to self-reinforced composites makes it possible to create complex 3D structures with improved mechanical performance. The result is an all-polyethylene compound that flows above the T_m of the HDPE matrix and therefore can be processed by classical thermoplastic processing methods, e. g. extrusion and injection molding.

As a result of the irradiation, the mechanical properties of the highly crystalline fibers deteriorate; thus, finding the appropriate gamma irradiation dose was crucial. Tensile tests and DSC analysis on single fibers were used to see the change in mechanical properties and crystallinity. Soxhlet extractions showed a decrease in gel fraction upon irradiation. Still, the fibers had significant gel fractions even after absorbing high doses due to the simultaneous effect of degradation and the favorable cross-linking. Cross-linking can improve the fibers' heat resistance, allowing them to withstand better the compounding and injection molding intact instead of forming a blend with the HDPE matrix.

Applying the fibers in a 20 %w/w content significantly improved the tensile properties. Among the composite samples, the 200 kGy absorbed dose gamma-irradiated fiber reinforced samples performed the best: in that case, the tensile strength and the modulus increased by 23% and 71%, respectively. The 41.1 MPa tensile strength, the 1.62 GPa tensile modulus, and the 64 Shore D hardness is quite similar to those of UHMWPE, which is widely used in implants, but the material introduced in this paper shows no issues with the melt flow characteristics. The *in vitro* cell studies showed that the composites and their components were not cytotoxic at all; the cells had a healthy shape and proliferated properly next to the supernatant of the samples; thus, no toxic component dissolved from the samples under physiological conditions.

Above the 200 kGy irradiation dose, further irradiation does not cause significantly higher cross-linking, likely because the reaction can only take place in the relatively small amorphous phase, and besides, the fibers tend to degrade too much. The results presented here have been achieved with a widely

available and productive manufacturing method, already available to many manufacturers. Considering the easy melt processing of the material, these gains are substantial and on par with the gains in other self-reinforced biomaterials. The results show the applicability of the self-reinforcing method presented here.

Declaration of Competing Interest

The authors declare that they have no known competing financial interests or personal relationships that could have appeared to influence the work reported in this paper.

Acknowledgments

The research reported in this paper was supported by the National Research, Development and Innovation Office (NKFIH FK 124147, FK 137749, FK 138501, FK 138501). László Mészáros and Kolos Molnár are thankful for János Bolyai Research Scholarship of the Hungarian Academy of Sciences, and for the ÚNKP-21-5 New National Excellence Program of the Ministry for Innovation and Technology. The research was further financed by the Higher Education Institutional Excellence Programme of the Ministry for Innovation and Technology in Hungary, within the framework of the Therapeutic Development thematic program of the Semmelweis University.

REFERENCES

[1] Ramakrishna S, Mayer J, Wintermantel E, Leong KW. Biomedical applications of polymer-composite materials: a review. Compos Sci Technol 2001;61:1189–224.
[2] Zhao ZN, Han B, Zhang R, Zhang Q, Zhang QC, Ni CY, et al. Enhancement of UHMWPE encapsulation on the ballistic performance of bi-layer mosaic armors. Compos B Eng 2021;221:109023.
[3] Cheng ZN, Li YL, Xu CX, Liu YY, Ghafoor S, Li FY. Incremental sheet forming towards biomedical implants: a review. J Mater Res Technol 2020;9:7225–51.
[4] Stepak B, Kobielarz M, Gazinska M, Szustakiewicz K, Pezowicz C, Antonczak AJ. ArF-excimer laser as a potential tool for manufacturing of biomedical polymeric devices. Express Polym Lett 2021;15:808–24.
[5] Kurtz SM, Devine JN. PEEK biomaterials in trauma, orthopedic, and spinal implants. Biomaterials 2007;28:4845–69.
[6] Hussain M, Naqvi RA, Abbas N, Khan SM, Nawaz S, Hussain A, et al. Ultra-high-molecular-weight-polyethylene (UHMWPE) as a promising polymer material for biomedical applications: a concise review. Polymers 2020;12:323.
[7] Brostow W, Hagg Lobland HE, Narkis M. Sliding wear, viscoelasticity, and brittleness of polymers. J Mater Res 2006;21:2422–8.
[8] Brostow W, Hagg Lobland HE. Materials: introduction and applications. John Wiley & Sons; 2017.
[9] Huang YF, Xu JZ, Li JS, He BX, Xu L, Li ZM. Mechanical properties and biocompatibility of melt processed, self-reinforced ultrahigh molecular weight polyethylene. Biomaterials 2014;35:6687–97.
[10] Drakopoulos SX, Psarras GC, Ronca S. Oriented ultra-high molecular weight polyethylene/gold nanocomposites: electrical conductivity and chain entanglement dynamics. Express Polym Lett 2021;15:492–502.
[11] Kurtz SM. UHMWPE biomaterials handbook: ultra-high molecular weight polyethylene in total joint replacement and medical devices. USA: Elsevier; 2016.
[12] Kmetty Á, Tábi T, Kovács JG, Bárány T. Development and characterisation of injection moulded, all-polypropylene composites. Express Polym Lett 2013;7:134–45.
[13] Vadas D, Kmetty Á, Bárány T, Marosi G, Bocz K. Flame retarded self-reinforced polypropylene composites prepared by injection moulding. Polym Adv Technol 2018;29:433–41.
[14] Kmetty Á, Bárány T, Karger-Kocsis J. Injection moulded all-polypropylene composites composed of polypropylene fibre and polypropylene based thermoplastic elastomer. Compos Sci Technol 2012;73:72–80.
[15] Kmetty Á, Bárány T, Karger-Kocsis J. Self-reinforced polymeric materials: a review. Prog Polym Sci 2010;35:1288–310.
[16] Bárány T, Izer A, Karger-Kocsis J. Impact resistance of all-polypropylene composites composed of alpha and beta modifications. Polym Test 2009;28:176–82.
[17] Megremis SJ, Duray S, Gilbert JL. Self-reinforced composite polyethylene (SRC-PE): A novel material for orthopedic applications, vol. 1346. ASTM Special Technical Publication; 1998. p. 235–55.
[18] Huang YF, Xu JZ, Xu JY, Zhang ZC, Hsiao BS, Xu L, et al. Self-reinforced polyethylene blend for artificial joint application. J Mater Chem B 2014;2:971–80.
[19] Venkatraman S, Kleiner L. Properties of three types of crosslinked polyethylene. Adv Polym Technol 1989;9:265–70.
[20] Zsíros L, Kovács JG. Surface homogeneity of injection molded parts. Period Polytech - Mech Eng 2018;62:284–91.
[21] Wunderlich B. Thermal analysis. Boston: Academic Press; 1990.
[22] Arnold JC. Evironmentally assisted fatigue. In: Milne I, Ritchie RO, Karihaloo BL, editors. Comprehensive structural integrity. London: Elsevier; 2003.
[23] Peacock A. Handbook of polyethylene: structure properties and applications. USA: Marcel Dekker; 2000.
[24] Firouzi D, Youssef A, Amer M, Srouji R, Amleh A, Foucher DA, et al. A new technique to improve the mechanical and biological performance of ultra high molecular weight polyethylene using a nylon coating. J Mech Behav Biomed Mater 2014;32:198–209.
[25] Elzubair A, Suarez JCM, Bonelli CMC, Mano EB. Gel fraction measurements in gamma-irradiated ultra high molecular weight polyethylene. Polym Test 2003;22:647–9.
[26] Wu XF, Wu C, Wang GL, Jiang PK, Zhang JQ. A crosslinking method of UHMWPE irradiated by electron beam using TMPTMA as radiosensitizer. J Appl Polym Sci 2013;127:111–9.
[27] Fan P, Cao Z, Zou HW, Luo LQ, Liu PB. Effect of gamma ray irradiation on processability and properties of ultra high molecular weight polyethylene. J Appl Polym Sci 2011;119:1542–7.
[28] Lombardo G, Bracco P, Thornhill TS, Bellare A. Crystallization pathways to alter the nanostructure and tensile properties of non-irradiated and irradiated, vitamin E stabilized UHMWPE. Eur Polym J 2016;75:354–62.
[29] Bellare A, Dorfman R, Samuel A, Thornhill TS. J-integral fracture toughness, Tearing modulus and tensile properties

of Vitamin E stabilized radiation crosslinked UHMWPE. J Mech Behav Biomed Mater 2016;61:493–8.
[30] Wang HL, Xu L, Li R, Hu JT, Wang MH, Wu GZ. Improving the creep resistance and tensile property of UHMWPE sheet by radiation cross-linking and annealing. Radiat Phys Chem 2016;125:41–9.
[31] Visco A, Richaud E, Scolaro C. Ageing of UHMWPE in presence of simulated synovial fluid. Polym Degrad Stabil 2021;189:109605.
[32] Hossain MI, Faisal HM, Tarefder RA. Determining effects of moisture in mastic materials using nanoindentation. Mater Struct 2016;49:1079–92.
[33] Juriga D, Laszlo I, Ludanyi K, Klebovich I, Chae CH, Zrinyi M. Kinetics of dopamine release from poly(aspartamide)-based prodrugs. Acta Biomater 2018;76:225–38.
[34] Bhattacharya R, Mukherjee K, Pal B. Polyethylene in orthopedic implants: recent trends and limitations. Reference module in materials science and materials engineering. Elsevier; 2021.
[35] Mamidi N, Leija HM, Diabb JM, Romo IL, Hernandez D, Castrejon JV, et al. Cytotoxicity evaluation of unfunctionalized multiwall carbon nanotubes-ultrahigh molecular weight polyethylene nanocomposites. J Biomed Mater Res 2017;105:3042–9.